FABRICATION AND CHARACTERIZATION OF HOLLOW MICRONEEDLE ARRAY USING DIFFRACTION UV LITHOGRAPHY

Jun Ying Tan¹, Albert Kim², and Jungkwun 'JK' Kim¹

¹Department of Electrical and Computer Engineering, Kansas State University, Manhattan, KS, USA, 66506 ²Department of Electrical and Computer Engineering, Temple University, Philadelphia, PA, USA, 19122

ABSTRACT

Hollow microneedles are extremely attractive to drug delivery domains with high demands from clinics and industry. However, its complicated fabrication processes have impeded its wide adoption. This paper presents a simple one-step fabrication method for hollow microneedles based on diffraction UV lithography and solid-liquid light propagation. The fabrication process utilizes bottom-up exposure of a liquid photosensitive resin through photomask patterns comprising a plurality of apertures. Hollow microneedles with various heights were fabricated in a range of 400 µm to 600 µm from a few minutes of UV exposure. The fabricated hollow microneedles were characterized with force-displacement tests showing a good tip strength of 0.35 N per single unit. A hollow fluidic test on a pig cadaver skin showed great potential for drug delivery. Also, batch fabrication with multiple height microneedles on a single substrate has demonstrated compatibility with the manufacturing process.

KEYWORDS

Hollow microneedles, diffraction UV lithography, liquid-solid light propagation, UV sensitive resin.

INTRODUCTION

With the advancement of micromachining techniques, microneedles have been frequently reported as a new drug delivery or sensing method [1] [2]. While little-to-no-pain and high drug delivery efficiency have been considered the advantages of microneedle kinds, a hollow microneedle has an additional unique feature of the integrated conduit. The capability to deliver a liquid state drug for treatment [3] or to derive such as body fluid for sensing [4] stands out from other types of microneedles. The conduit allows hollow microneedle to deliver heavier molecular compounds such as proteins, hormones, and vaccines. Recent studies have reported successful vaccine delivery cases using hollow microneedles and the benefits of using hollow microneedles over hypodermic needles [5].

However, manufacturing such hollow microneedles remained challenging compare to other types of microneedles. A high-end excimer or fiber laser machining reported several successful fabrications of the hollow microneedles. However, the fabrication typically requires a sequential process with precise alignment, which restrains low-cost batch manufacturing [6] [7]. On the other hand, a conventional photolithography-based hollow microneedle fabrication demonstrated batch process capability. However, a long process time (e.g., 10-hour soft bake) and several mask alignments diminished the benefits of low-cost and simple fabrication [8] [9].

The previous work demonstrated a 30-minute start-tofinish process of a solid microneedle fabrication using diffraction lithography [10]. In this paper, we present hollow microneedle fabrication based on expanded diffraction lithography. The advanced fabrication processes utilize a diffraction phenomenon when light passes through the micro patterns and its internal reflection due to liquid-to-solid transition in photosensitive resins, as illustrated in Figure 1. The micropatterns consist of an outer window pattern and an opaque inner pattern (i.e., a ring shape). When collimated UV light encounters such photo patterns, the opaque inner pattern forms the conduit of the hollow microneedle while the outer pattern crosslinks the sidewall. Adjusting the positions and the shapes of the inner pattern within the outer window could also create various shapes of the hollow microneedles. The proposed direct UV exposure to the liquid photosensitive resin creates a sharp tip and a smooth sidewall profile, which is distinguished from the other report [9]. Since the proposed fabrication method is simple, rapid, and batchprocess compatible, various practical applications using the hollow microneedle are expected, including bio-sensing and drug delivery fields.

FABRICATION

The fabrication process of the hollow microneedles comprises two parts: (1) through-hole substrate and (2) hollow microneedles, as illustrated in Figure 2. The fabrication of through-hole substrate started with a circular opaque patterned photomask (Photomask 1) prepared using a maskless projection lithography system (SF-100 XPRESS, Scotech LTD.), as shown in the inset image in

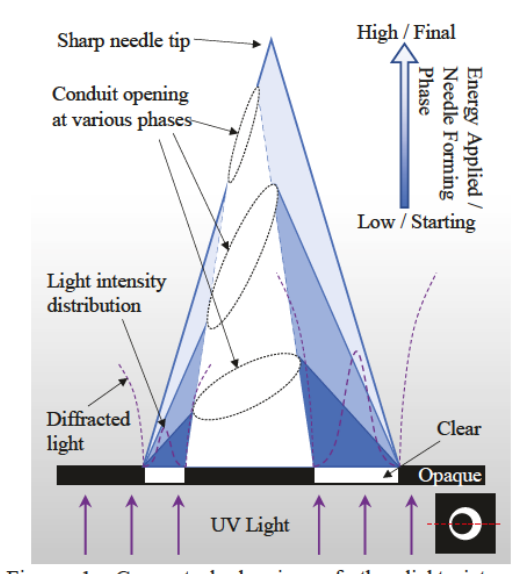


Figure 1. Conceptual drawing of the light intensity distribution through a photopattern with an outer windowed pattern and a left-shifted inner opaque pattern.

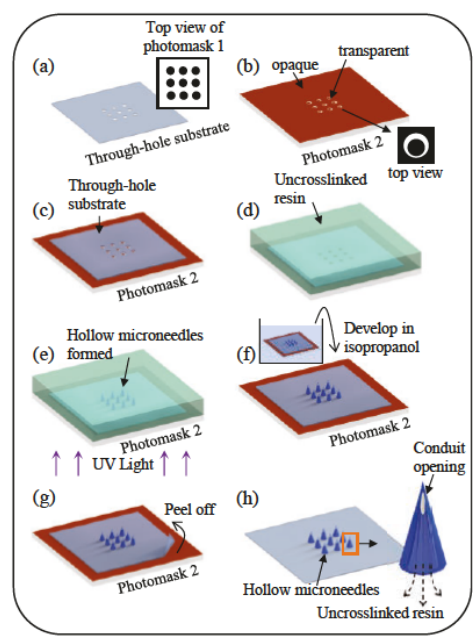


Figure 2. Fabrication process of hollow microneedles array.
(a) through-hole substrate, (b) photomask 2 design, (c) through-hole substrate alignment on the photomask 2, (d) uncrosslinked resin coating and thermal reflow process, (e) backside UV exposure, (f) first development process, (g) through-hole substrate detachment process, (h) second development and hollow microneedles array is complete.

Figure 2(a). The photomask 1 was spin-coated with photosensitive resin (Surgical guide resin, Formlabs, Inc.) at 1,000 rpm for 30 seconds, then allowed reflow gradually, resulting in a final thickness of 130 µm. Then, backside UV exposure (H-line) was performed, followed by a development process in isopropanol. The crosslinked resin was detached from photomask 1, thereby completing the through-hole substrate, as shown in Figure 2(a).

Another photomask (Photomask 2) was prepared using the same projection lithography system as illustrated in Figure 2(b). The photomask 2 design is shown in the inset image of Figure 2(b). The through-hole substrate was aligned on photomask 2 (Figure 2(c)). The sample was coated with photosensitive resin, and the final thickness of the resin was 1 mm. Backside UV exposure was performed (Figure 2(e)), followed by the development process in isopropanol with mild agitation for 5 minutes (Figure 2(f)). The through-hole substrate, along with the hollow microneedles, was peeled off from the photomask 2 (Figure 2(g)). Since the microneedles and the substrate shares the same core material, the bonding strength was strong. They stayed intact while peeling off photomask 2 from the microneedles. The sample was further cleaned with the isopropanol alcohol and dry to complete the hollow microneedle array, as shown in Figure 2(h).

RESULTS

The conduit opening size, the tip profile, and the needle height are the important characteristics of hollow microneedles as they determine the functionality and mechanical stability of the hollow microneedles. In the

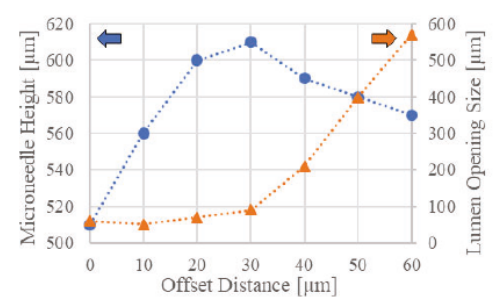


Figure 3. Relationship of the inner pattern offset distance with the microneedles height and the conduit opening size.

proposed fabrication method, these characteristics are mainly defined by five parameters: diameters of outer and inner patterns, offset distance of the inner pattern from the center, UV source intensity, and total UV exposure energy. The location of the inner pattern within the outer pattern dictates the shapes of hollow microneedles. In this paper, we extensively study the effect of such offset distance of the inner pattern while other parameters were fixed: the diameters of the outer and inner patterns were designed to be $300 \ \mu m$ and $175 \ \mu m$, respectively. The UV intensity was set at $1.85 \ mW/cm^2$ and the total UV exposure energy was fixed at $148 \ mJ/cm^2$ (exposure time = $80 \ secs$).

Figure 3 describes the fabrication relationship in control of the offset distance of the inner pattern from the center of the outer pattern. The hollow microneedles height and the conduit opening size were measured and recorded for every 10 μ m increment of the offset distance. The hollow microneedles reach the tallest height of 610 μ m when the offset distance is at 30 μ m, then gradually decrease when the offset distance becomes larger. The conduit opening size remains relatively constant under 100 μ m when the offset distance ranges from 0 to 30 μ m, then drastically increases when the offset distance becomes larger.

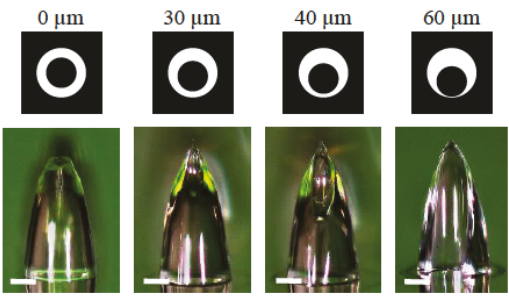


Figure 4. Optical image that shows the results of the hollow microneedles with 0, 30, 40 and 60 μ m offset distance. Scale bar = 100 μ m.

Figure 4 shows the fabrication results of the hollow microneedles using 0, 30, 40, and 60 μm offset distance of the inner pattern. The 0 μm (center alignment) offset sample demonstrated an example of the first type of hollow microneedles, i.e., a uniform hollow microneedle with a blunt tip and centered conduit opening with a size of 90 μm . The samples fabricated with 30 and 40 μm offsets demonstrated sharp needle tips, and the conduit opening formed at the needle sidewall with the size of 90 μm and 210 μm , respectively. The 60 μm offset sample shows a

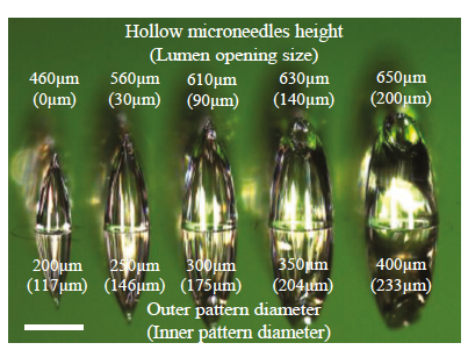


Figure 5. Various type of the hollow microneedles fabricated on single photomask using single UV exposure. *Scale bar* = 300 um.

hollow microneedle with a sharp tip and a wide conduit opening.

Based on the results shown in Figure 4, the 30 µm offset design was carried out for the subsequent fabrication parameter investigation, the scaling effect. While we maintain the ratio of inner and outer diameter to be around 0.58, the photo pattern was scaled proportionally to have an outer diameter of 200, 250, 300, 350, and 400 µm and the inner diameter of 117, 146, 175, 204, and 233 µm, respectively. The five photo patterns were prepared on a single photomask, used for hollow microneedles fabrication as described above. The results are shown in Figure 5. Given the same exposure energy, the hollow microneedle height increased linearly as a function of outer pattern diameter, suggesting a direct relationship between the microneedle height and the outer pattern diameter. Similarly, the conduit opening size also showed an increasing trend with the inner pattern diameter. Additionally, this result demonstrated that our fabrication process could create various types of hollow microneedles using a single photomask with a single exposure process.

We also demonstrated the batch manufacturability and reliability of the proposed fabrication process. Figure 6 shows results of an array of hollow microneedle fabrication using a photomask with a 20 by 20 ring shape photo pattern array; an outer pattern diameter was 300 μ m and an inner pattern diameter was 175 μ m. Hollow microneedles array was successfully fabricated with an average height of 515 μ m and an average conduit opening size of 230 μ m.

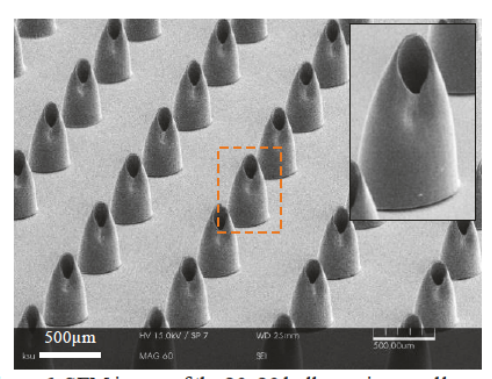


Figure 6. SEM image of the 20x20 hollow microneedles array with outer pattern diameter of $300~\mu m$, average height of $515~\mu m$ and average conduit opening of $230~\mu m$.



Figure 7. Optical image of 4x4 hollow microneedles array for mechanical test.

MECHANICAL EXAMINATIONS

To examine the functionality of the hollow microneedles, we conducted a liquid ejection test, skin penetration test, and the force-displacement test. To validate the consistency of the testing results, three sets of 4 x 4 hollow microneedles array were prepared and used throughout the experiments. Each hollow needle had a bottom diameter of 300 μ m, a height of 600 μ m, and a conduit opening size of 100 μ m, as shown in Figure 7.

Liquid Ejection Test

A liquid ejection test confirms the hollow cavity of the microneedles array. To test the liquid ejection, the microneedles array was installed on a custom-made blue ink reservoir, which was then secured with four screws at the four corners (Figure 8(a)). The reservoir was refillable by a connected syringe pump. When the syringe was driven at a rate of 200 ml/hr, the microneedle could successfully eject 13 visible streams of blue ink out of 16 units (yield > 80%), as shown in Figure 8(b). The liquid ejection test was also conducted underwater with the same driving rate. When the microneedle prototype was driven with the same pumping rate (via a syringe pump), it could eject the ink approximately 2 cm from the water surface (Figure 8(c)).

Skin Penetration Test

The skin penetration test was assessed using pig cadaver skin. The 4x4 hollow microneedles array was placed on top of the pigskin, facing downwards, then compressed using thumb pressure towards the skin to insert the hollow microneedles array into the skin. The inserted

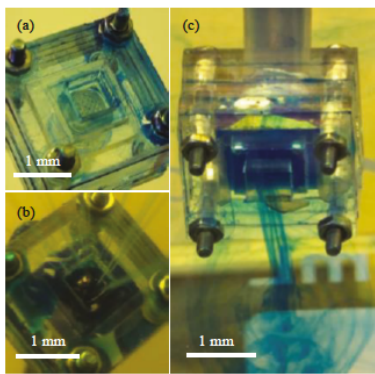


Figure 8. Optical image of the result of liquid ejection test. (a) Before liquid ejection test in air, (b) liquid ejection test in air, (c) liquid ejection test under water.

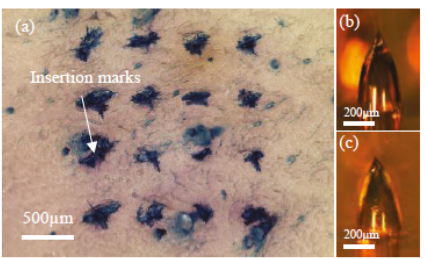


Figure 9. Results of the skin penetration test. (a) Pigskin with insertion marks, (b) before, and (c) after insertion.

area was stained with blue tissue marking dye for visualization (Tissue marking dye, Cancer Diagnostics Inc.). Figure 9(a) shows the results of the skin penetration test. 16 visible blue marks were observed on the skin, suggesting 100% successful insertion. Figure 9(b-c) shows an example of a single unit of hollow microneedle before and after insertion. Slight deformation occurred at the tip, but no visible damage or fracture was observed at the conduit opening and the needle body.

Force Displacement Test

The microneedles array was mounted on a platform facing upwards. A force gauge (FC200, Torbal Inc.) was installed on a motor-integrated threaded rod that was controlled by a microcontroller (Arduino UNO Rev 3, Arduino). The force gauge was programmed to move downwards at a speed of 1.2 mm/min until it has fully compressed the tip of the hollow microneedles. The force-displacement graph is shown in Figure 10, where a peak force was measured to 0.35 N per needle which is suitable for the skin penetration (higher than the typical force requirement of 0.2 N). The optical images on the right show the side view of the hollow microneedle before and after the force displacement test.

CONCLUSION

A simple, low-cost, rapid diffraction UV lithography-based hollow microneedles fabrication method is proposed and demonstrated. Various types of hollow microneedles were successfully fabricated by applying a small change in the photo pattern. The 4 by 4 hollow microneedle arrays with a base diameter of 300 μ m, a height of 600 μ m, and a conduit opening size of 100 μ m were fabricated and tested.

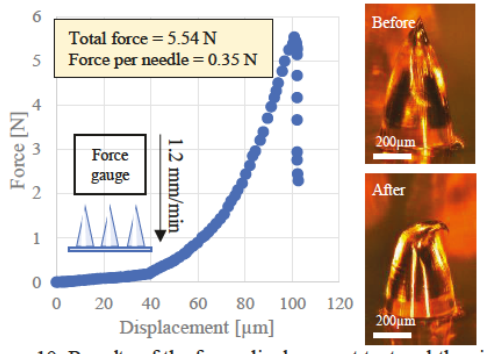


Figure 10. Results of the force displacement test and the side view of the microneedles before and after test

The tested microneedles array was successfully inserted into pigskin without visible damage and showed up to 0.35 N per needle tip. A 20x20 hollow microneedles array was fabricated, which demonstrated the batch process capability for manufacturing.

ACKNOWLEDGEMENTS

This work has been supported by a grant (ECCS-2029086 and ECCS-2029077) from the National Science Foundation of the United States.

REFERENCES

- [1] Z. Zhao, Y. Chen, and Y. Shi, "Microneedles: a potential strategy in transdermal delivery and application in the management of psoriasis," RSC Adv., vol. 10, no. 24, pp. 14040–14049, Apr. 2020.
- [2] Y.-C. Kim, J.-H. Park, and M. R. Prausnitz, "Microneedles for drug and vaccine delivery," Adv. Drug Deliv. Rev., vol. 64, no. 14, pp. 1547–1568, Nov. 2012.
- [3] A. S. Rzhevskiy, T. R. R. Singh, R. F. Donnelly, and Y. G. Anissimov, "Microneedles as the technique of drug delivery enhancement in diverse organs and tissues," *J. Controlled Release*, vol. 270, pp. 184–202, Jan. 2018.
- [4] L. Xie, H. Zeng, J. Sun, and W. Qian, "Engineering Microneedles for Therapy and Diagnosis: A Survey," *Micromachines*, vol. 11, no. 3, Art. no. 3, Mar. 2020.
- [5] K. van der Maaden et al., "Novel Hollow Microneedle Technology for Depth-Controlled Microinjection-Mediated Dermal Vaccination: A Study with Polio Vaccine in Rats," Pharm. Res., vol. 31, no. 7, pp. 1846–1854, Jul. 2014.
- [6] J. Chen et al., "A Minimally Invasive Hollow Microneedle With a Cladding Structure: Ultra-Thin but Strong, Batch Manufacturable," *IEEE Trans. Biomed. Eng.*, vol. 66, no. 12, pp. 3480–3485, Dec. 2019
- [7] D.-S. Lee, C. G. Li, C. Ihm, and H. Jung, "A three-dimensional and bevel-angled ultrahigh aspect ratio microneedle for minimally invasive and painless blood sampling," *Sens. Actuators B Chem.*, vol. 255, pp. 384–390, Feb. 2018.
- [8] P. Wang, S. Paik, S. Kim, and M. G. Allen, "Hypodermic-Needle-Like Hollow Polymer Microneedle Array: Fabrication and Characterization," J. Microelectromechanical Syst., vol. 23, no. 4, pp. 991–998, Aug. 2014.
- [9] P. Dardano, S. De Martino, M. Battisti, B. Miranda, I. Rea, and L. De Stefano, "One-Shot Fabrication of Polymeric Hollow Microneedles by Standard Photolithography," *Polymers*, vol. 13, no. 4, Art. no. 4, Jan. 2021.
- [10] J. Y. Tan, M. Ahn, H. Al-Thuwaini, S. Choi, and J. J. K. Kim, "Diffraction Lithography for 3-D Microneedle Fabrication," in 2020 IEEE 33rd International Conference on Micro Electro Mechanical Systems (MEMS), Jan. 2020, pp. 921–924.

CONTACT

*JK Kim, tel: +1-785-370-0917; jkkim1324@ksu.edu